

An *in-situ* hot stage for temperature-dependent tapping-mode™ atomic force microscopy

S. G. Prilliman, A. M. Kavanagh, E. C. Scher, S. T. Robertson, K. S. Hwang, and V. L. Colvin^{a)}

Department of Chemistry and Center for Nanoscale Science and Technology, Rice University, Houston, Texas 77005

(Received 26 May 1998; accepted for publication 23 June 1998)

Tapping-mode atomic force microscopy (TM-AFM) is a widely used method for the study of the nanometer scale morphology of soft materials such as biological samples and polymers. Many of these materials have structures and properties which are a sensitive function of temperature even below 100 °C making the control of temperature in such an instrument quite valuable. This paper describes the construction of a heater for a commercial TM-AFM which can reach surface temperatures as high as 100 °C. Temperature variations affect many experimental parameters in an atomic force microscope, and to compare images collected at different temperatures it is critical to evaluate these instrumental effects. In particular, the cantilever resonance frequency decreases as samples become hot; this effect is easily corrected by frequently resetting the drive frequency at high temperatures. As an example of the utility of this technique images of the nanoscale changes that occur prior to the bulk melting of paraffin crystals are presented. © 1998 American Institute of Physics. [S0034-6748(98)04209-9]

I. INTRODUCTION

Atomic force microscopy (AFM) is becoming a widely used technique for imaging soft materials with nanometer scale resolution.^{1(a),1(b),2} Compared to other microscopies, such as scanning and transmission electron microscopy, force microscopy permits samples to be studied under ambient conditions without special sample preparation. This not only makes imaging more routine, but it also provides for microscopy conditions more representative of real-world applications. In the special case of soft materials a new variant of force microscopy, tapping-mode atomic force microscopy (TM-AFM), has been developed to minimize mechanical damage to the samples.^{3(a),3(b),4} It works by vibrating a probe tip at megahertz frequencies near its resonance and detecting topography through changes in the probe's amplitude of vibration. While the probe does contact the surface in this method, its contact times are very short and little to no lateral motion occurs during the contact period.⁵⁻⁷ The applications of TM-AFM to the study of numerous soft materials such as polymers^{8,9} and biological systems^{10,11} have grown enormously over the last few years as commercial atomic force microscopes with tapping-mode capability have become available.

The prospect of controlling sample temperature while simultaneously imaging a material extends the potential of any microscopy. Controlled temperature studies have been recently carried out for contact mode AFM in air and under controlled atmosphere conditions.¹²⁻¹⁴ However, the ability to heat in TM-AFM under ambient conditions would be particularly advantageous since softer materials experience a di-

verse array of structural and phase changes over relatively narrow temperature ranges. For example, in one recent report temperature-dependent TM-AFM was used to image siloxane phase transitions below room temperature.¹⁵ As a function of temperature the morphology of thermotropic structures was identified using the phase imaging abilities of TM-AFM. There are few other examples of the use of temperature control in TM-AFM despite its numerous applications. This is in part due to the technical difficulties faced when integrating a hot stage into a force microscope, especially one that operates under ambient rather than vacuum conditions.

Hot stage designs for contact-mode force microscopes can serve as a departure point for the construction of tapping-mode hot stages. Musevic *et al.* describe in detail a design for a resistive heater controlled by a homebuilt feedback circuit for use in a commercial contact-mode AFM.¹⁶ Warming of the microscope components, in particular the scanning stage which sits below the sample, was a limitation of their design and apparently lead to image distortions at elevated temperatures. A similar heater design was introduced by Baekmark *et al.*¹⁷ They used a thin piece of glass for heater insulation and obtained atomic resolution images of graphite up to 52 °C. In another example of a contact-mode heater AFM a Peltier cooler was used to keep the scanning piezotube from warming during sample heating. This arrangement allowed for high resolution contact-mode images to be collected up to 95 °C.¹⁸ These examples demonstrate the utility of resistive heating in force microscopes and illustrate the importance of adequate insulation of the hot stage.

The goal of this work is to extend the use of hot stages to tapping-mode atomic force microscopy. A description of a resistive heater designed for use in one of the most widely

^{a)}Author to whom all correspondence should be addressed; electronic mail: colvin@ruf.rice.edu.

available atomic force microscopes, a Digital Instruments Nanoscope III, is provided in the experimental section. Its construction and routine use has been simplified by using a commercial thermal controller to set and maintain the temperature. While the basic form is adapted from a heater built for contact-mode AFM,¹⁶ the useful temperature range has been extended by the incorporation of effective thermal insulation. This paper also addresses a number of important issues concerning the effects that heating has on the operation of the tapping-mode force microscope. In particular, the resonance curve of the force microscope probe, or cantilever, changes as the sample surface heats. This requires that the microscope be retuned at regular intervals while at high temperatures. With regular monitoring of this issue, high quality images of soft materials are possible at temperatures as high as 100 °C.

II. EXPERIMENT

Like many of the contact mode heaters this hot stage employs resistive heating as a source of heat. A film of indium-tin-oxide (ITO) is used as a conductive element in this design since it is robust, spatially uniform, and commercially available. A 0.64-cm-thick sheet of glass coated on one side with a thin layer of indium-tin-oxide (ITO) (Applied Films Corporation, Boulder, CO) was cut into 1 cm square pieces. In order to assure even electrical conduction across the heater, gold was evaporated onto the ITO side with a 6-mm-wide strip of tape covering the middle part of the squares, which upon removal left gold strips of 2 mm on either side. A thin platinum RTD (Omega Engineering, Stamford, CT) with 60 cm of 30 gauge lead wires soldered to the existing leads was then mounted on the ITO side of the squares with thermally conductive epoxy (Omegabond 101, Omega). In contrast to previously published heater designs,¹⁶ silver epoxy (Chemtronics Inc., Kennesaw, GA) was found to be acceptable for affixing 60 cm 30 gauge wires to the gold strips. To insulate the AFM probe tip against electric fields, a piece of copper foil tape was fastened to the insulating side of the glass. It was necessary to color the foil with a black marker in order to prevent reflection of the positioning diode laser while in the AFM. The total resistance across the heater was approximately 50 Ω to ensure a match to the thermal controller. Current and temperature feedback were provided by a Lakeshore 330 Thermal Controller (Lakeshore, Westerville, OH) [see Fig. 1(A)]. This controller when used with a platinum resistive thermal detector (RTD) has an accuracy of ± 0.08 °C.

It is necessary to thermally insulate the heater from the piezoelectric devices located below the sample stage in the Nanoscope III. This was accomplished by bonding a low-thermal conductivity epoxy (Omegabond 100, Omega) to a 1 cm \times 1 cm \times 2.5 mm piece of balsa wood to the underside of the heater. Another piece of balsa wood of the same size was affixed to the first piece with the grain of the wood pieces oriented perpendicular to each other. Balsa wood was chosen because of its rigidity and extremely low thermal conductivity (0.57 W/m °C) across the grain, versus 1.46 W/m °C for MacorTM.^{19,20} Finally, a 15-mm-diam AFM puck

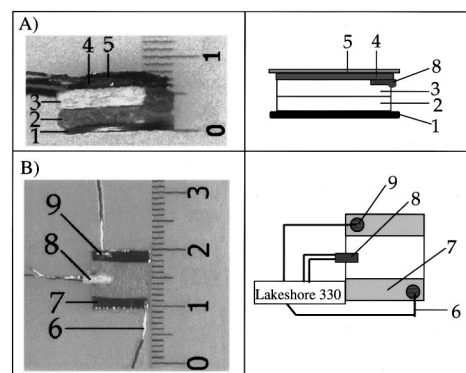


FIG. 1. Photograph and schematic of TM-AFM heater. (A) A side view of the TM-AFM heater illustrating the thickness and components of the system. 1—Metal sample holder puck. 2—First layer of balsa wood. 3—Second layer of balsa wood with grain perpendicular to the first 4: ITO coated glass. 5—Copper foil. (B) A top view of the heater. 6—Wires for resistive heating (connected to the Lakeshore 330). 7—Gold strips for even electrical conduction. 8—Resistive thermal detector (RTD) for feedback control (connected to the Lakeshore 330). 9—Silver conductive epoxy (scale in centimeters.)

(Ted Pella, Redding, CA) was attached to the second piece of balsa wood and served to hold the heater to the magnetic sample stage. The final heater was 7.7 mm thick as opposed to the 5-mm-thick heater used recently in contact mode operation.¹⁸

The sample surface temperature was calibrated against the RTD mounted directly on the conducting heating element by Stokes/anti-Stokes Raman spectroscopy of a piece of silicon mounted on top of the heater (Fig. 2).^{21,22} Though this measurement gives a precise measure of real surface temperature, the error associated with the integration of the Raman features was large. To achieve better accuracy, as well as to measure temperatures directly in the microscope, a thermocouple mounted directly to the top silicon surface was also used for calibration (Fig. 2).

Images were taken on a Nanoscope III Multi-Mode AFM (Digital Instruments, Santa Barbara, CA) with Nano-probe TESP tips (Digital Instruments) with resonance frequencies between 290 and 346 kHz. Samples were scanned at rates between 1.5 and 3.0 Hz. All images shown here were obtained using the “J” piezotube scanner which has a maximum scan size of 125 by 125 μ m. Some lateral sample drift is always encountered during imaging over the span of hours even when not heating samples. To account for this the x and y sample position were routinely changed to keep features centered.

Because of the relatively large thickness of the heater, it was necessary to use a 6.3 mm tall “spacer” to create enough clearance to mount the heater on the sample scanner. This spacer was a ring of 6.3-mm-thick aluminum which was machined to curve around the sample scanner tube and raise the AFM head.

The heater was found to expand upon heating, and if the tip was engaged with the surface this expansion could break the cantilever. In order to avoid this, two precautions were taken. First, the heater was ramped at a rate between 2 and 5 °C/min from the initial to final temperature. Second, the z -center position was closely monitored and the step motor

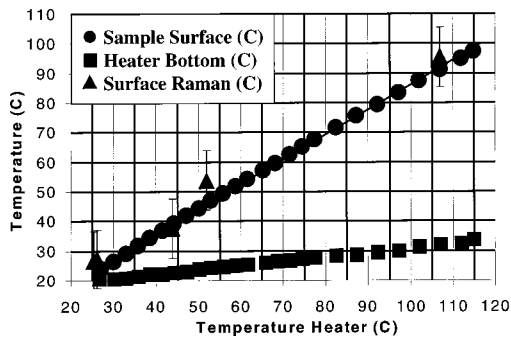


FIG. 2. External calibration of the TM-AFM heater. A thermocouple mounted directly to the top of a silicon sample was used to calibrate the heater surface temperature against the heating element temperature (●). The measurement was repeated five times with a heater positioned in the TM-AFM system in a fashion identical to that used during imaging. The error bars represent twice the standard deviation of these external calibrations. These temperatures were verified using the ratio of the anti-Stokes to Stokes Raman scattering of the silicon substrate (▲) collected on a heater mounted outside of the AFM. Also shown is the temperature of the bottom of the heater (■) as measured by a thermocouple.

was used to move the tip up when it neared its retracted limit. Alternatively the tip could be retracted during heating and upon reengagement would reach an appropriate height. The AFM was placed under a neoprene cover on an isolation tripod in order to eliminate vibrations being transmitted by the heater lead wires to the AFM sample stage and to provide thermal stability.^{3(c)}

All samples were prepared on silicon wafer chips. The paraffin crystals were made by dissolving high purity $C_{33}H_{68}$ (Aldrich, 98+%) in petroleum ether (10^{-4} M) and allowing this solution to dry on clean silicon.²³ The number and size of the crystals were controlled by varying the solution concentration. An AFM replica grating was purchased from Ted Pella and was specified to have a grating spacing of 463 ± 6 nm or 2160 lines/mm.

III. RESULTS

This heater provides stable and reproducible temperature control on the sample stage from room temperature to 100 °C (Fig. 2). In these data the temperature of the heater itself is compared to the surface temperature as measured by a thermocouple mounted on a silicon substrate and verified by Stokes/anti-Stokes Raman scattering from the silicon sample. Response times of the heater were quite rapid: stable surface temperatures were observed after only 1 min. From Fig. 2 it is apparent that the temperature of the heating element is approximately 13% higher than the temperature of the sample surface. This temperature drop was reproducible with several different heaters mounted identically inside the AFM housing. In addition, data were collected from regions near the middle and edge of the sample with no difference in the observed results.

Figure 3 shows the image of a replica grating collected at room and high temperatures. For this experiment the cantilever remained in contact with the sample at all times during heating; the primary adjustment for higher temperatures involved the use of the z stepper motor to pull the tip away from the expanding sample. The spacing of this AFM cali-

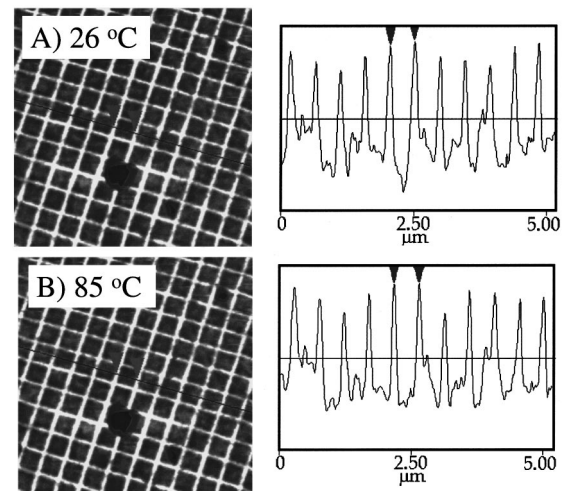


FIG. 3. Force microscopy image of a calibration sample at room and high temperature. (A) This room temperature image ($5 \mu\text{m}$ in x and y) of a grating replica shows the typical resolution of a TM-AFM and serves to calibrate the x and y piezoelectric scanners. The inset is a cross section taken along the line shown. The distance between the two arrows in the section is 468.8 nm, in good agreement with the manufacturer's reported grating spacing of 463 ± 6 nm. The large hole is a defect in the sample and was intentionally included in the image to serve as a reference point for sample drift. (B) At high temperatures the image looks identical to room temperature; the inset shows a grating spacing of 468.8 nm. The hole has remained in the same position though some manual adjustment of the x and y position was necessary. The z scale in both cases is $50 \mu\text{m}$ and the lateral scan size is $5 \mu\text{m}$.

bration standard, 468.8 nm, is identical at both temperatures. This result illustrates the stability of the piezoelectric positioning elements at high temperatures. Also, the images recorded at high temperatures show good contrast and sharp features. As will be discussed, quality images at high temperatures are only possible if the changes in the microscope operation at elevated temperatures are accounted for.

The most important change in the microscope itself at high temperature is the systematic variation in the resonance curve of the cantilever (Fig. 4). To evaluate this phenomenon the tip was used to image a hot sample surface for 10 min. It was then placed approximately $20 \mu\text{m}$ above the sample surface using the sample stage stepper motors and the resonance

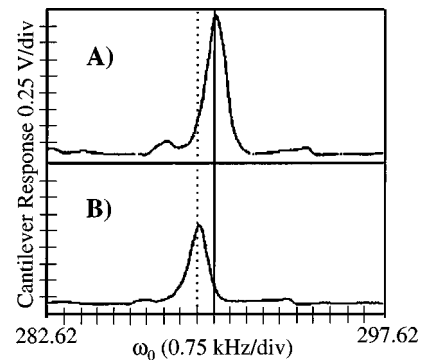


FIG. 4. Cantilever resonance curve at room and high temperatures. (A) At room temperature the cantilever resonance curve shows a peak at 290.12 MHz (the black solid line). For imaging with this tip the drive frequency was set just below the peak at 290 MHz. (B) At high temperatures the resonance frequency shifts downwards to 289.48 MHz (dashed line), the peak broadens, and the overall resonance width increases. Resetting the drive frequency and amplitude at high temperatures is necessary to obtain quality images.

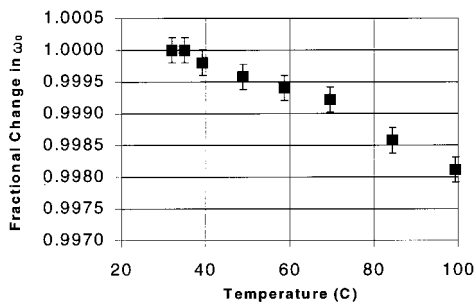


FIG. 5. Shift of resonance frequency with temperature. The fractional shift in resonance frequency with temperature is constant among different cantilevers and tip holders as indicated by these data. Though the percentage shift is small over the range of this heater, the relatively narrow resonance widths mean that these small changes have profound effects on the position of the drive frequencies necessary for quality images.

frequency of the cantilever was quickly determined. At this distance from the surface the tip is free from sample interactions and the frequency and width of its resonance response depends only on cantilever force constant and mass. At high temperatures the resonance frequency of silicon cantilevers decreases and the width of the resonance increases. These changes were qualitatively similar for different cantilever types as well as tip holders. The shift of the cantilever frequency was especially consistent and moved downwards with increasing temperature (Fig. 5); changes in resonance width were more variable mainly due to the presence of multiple resonances in some tips, but the general observation of broadening was consistent.

The behavior of the free amplitude of the cantilever vibration was not as predictable. In the example shown in Fig. 4 at high temperatures the tip was driven with the same amount of drive voltage, or drive amplitude, as at low temperatures; however, its resulting oscillation was not as large at high temperatures. Other tips show different changes in free space amplitude at high temperatures.

IV. DISCUSSION

While Fig. 3 illustrates the stability of this hot stage design at high temperature, there are a number of technical issues faced when integrating a hot stage into a force microscope. This section discusses three of these issues: accurate measurement of sample surface temperature, insulation of the heating element from the microscope, and optimization of imaging conditions at high temperatures.

The measurement of sample surface temperature in a force microscope hot stage is problematic as the microscopy requires physical contact between probe tips and the surface. This prevents direct attachment of thermocouples to the sample surface and thus requires that sample surface temperature be calibrated against the temperature reading of the heater itself. Such a calibration is illustrated in Fig. 2, which shows that the sample surface temperature is systematically lower than the temperature of the heating element itself. The $\sim 13\%$ temperature drop is not surprising given that the resistive heating surface is separated from the sample surface by 0.6 mm of glass (Fig. 1).

Repeated measurements of the surface versus heater temperature indicate that the temperature drop across the glass plate is quite reproducible. An important issue, however, in calibration of these heaters is the need for the systems to be evaluated inside of the microscope itself. In particular, an accuracy on the order of $\pm 2^\circ\text{C}$ can be achieved if the position of the tip holder relative to the sample surface is held to less than 1 mm. This allows the surface temperature to be determined during tests in which the sample is not actually imaged. Outside of the microscope altogether, in an environment free of external heat sinks, the average temperature drop between the surface and heating element was 8.5%, as opposed to 13% in the microscope. This indicates the heat loss to the elements of the hot stage itself is at least as important as heat loss to the tip holder and other microscope components.

While the physical separation between the heating element and the sample surface does have disadvantages with respect to temperature measurement, its inclusion in the design was motivated by practical considerations. The use of glass coated with indium-tin-oxide as a resistive heating element provides a physically stable and uniform conducting surface. The plain glass underside of these sheets provides an ideal sample platform which is inert, easily cleaned, and can be modified for a variety of sample types. In addition, the electrical connections to the heating element are delicate and must be shielded from the force microscope electronics. The presence of the glass insulates the heater both mechanically and electrically from the force microscope system.

One important feature of the hot stage design presented here is the thermal insulation between the heating element and the sample mount. Figure 2 shows the temperature of the bottom of the heater versus heating element temperature. It is important that this temperature remain low since the heater rests directly on the thermal piezoelectric tube responsible for $x-y$ sample positioning. Excessive heating of these components not only causes distorted images, but also may lead to depoling of the piezoelectrics. With appropriate insulation the temperature of the heater bottom will not rise more than 10° , which is an acceptable temperature rise for good images. Two parameters controlled the success of the thermal insulation: the thickness of the insulating layer and the nature of the thermal insulation. While thick insulation layers afforded better insulation, the overall heater thickness was limited to 6 mm. Heaters thicker than this would not stay affixed to the rapidly scanning piezotube and distorted images would result.

In order to obtain the best insulation in the available space a number of different materials were screened for use as insulation including thermally insulating ceramics, StyrofoamTM, fiberglassTM cloth, cork, and balsa wood. Fiberglass cloth was not suitable for this application as it was not rigid enough to maintain a constant position during the lateral motion of the sample during scanning. Styrofoam provides excellent thermal insulation but it undergoes a glass transition at 100°C which limits the useful temperature range of the heater. Thermally insulating ceramics, on the other hand, proved to be poor insulators relative to cork and balsa wood. Balsa was the final choice because of its rigidity, low thermal

conductivity, and its anisotropic thermal properties. By stacking two layers of balsa with grains running perpendicular to each other, the overall conductivity was made extremely low.

The importance of hot stage insulation in this particular example is a direct result of the design of the Digital Instruments force microscope; other manufacturers achieve x - y scanning by moving the tip rather than the sample holder, and for these configurations insulation of the sample bottom would be less important. Instead, insulation of the area above the sample surface, where the tip and its controlling piezoelectrics are situated would be critical for these systems. Such thermal shielding would require some limitation of the access of the tip to the surface and might prove difficult to implement.

The presence of a hot sample surface changes the operation of a tapping mode force microscope and these changes must be accounted for before temperature-dependent data can be interpreted. Tapping-mode force microscopy works by driving a silicon cantilever at frequencies just below its resonance; changes in the sample topography are detected through changes in the amplitude of the cantilever resonance. Given this detection method, the exact drive frequency of the cantilever relative to its natural frequency is a crucial issue in image formation and analysis.²⁴⁻²⁷ In the Nanoscope III TM-AFM resonance curves can be collected on any tip allowing the user to visualize the cantilever behavior and choose, or ‘tune’ the drive frequency accordingly. Figure 4 shows two representative resonance curves at low and high temperatures. Typical drive frequencies would be chosen to lie at lower frequencies than the peak where the amplitude is only 80% of its maximum value. As the cantilever warms as a result of its proximity to the hot sample surface, its force constant decreases. This has two effects: first, it lowers the resonance frequency of the cantilever and second, it increases the resonance width. The first of these changes, the depression of the cantilever oscillation, is quite reproducible (Fig. 5).

The third change in cantilever resonance with temperature is the change in the net amplitude of the vibration. In some situations the tip experiences larger oscillations at high temperatures and in other cases smaller oscillations (as shown in Fig. 5). The amplitude of the vibrating tip depends on a number of complex factors including the tip reflectivity, the contact between the tip and the driving piezoelectric, and the voltage response of the driving piezoelectric. Thermocouples mounted directly to the metal block of the tip holder near the piezoelectric elements responsible for driving tip oscillation indicate that this component can reach temperatures of 40–50 °C when surface temperature is 100 °C. This is not surprising since this piece sits approximately 1 mm above the surface and is not insulated from the heater. This temperature rise might be enough to alter the response function of the driving piezoelectric and thus change the observed amplitude of the cantilever.

These changes in the cantilever properties with temperature can be easily accounted for by frequent tuning while the sample surface is hot. Figures 3(A) and 3(B) show images collected of the calibration grating at room temperature and

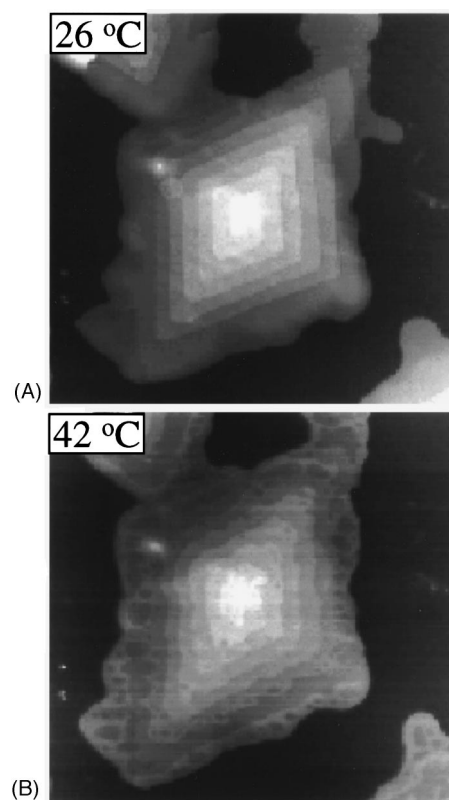


FIG. 6. Images of paraffin crystals at high temperature and room temperature. (A) At room temperature, paraffin samples exhibit striking diamond-shaped crystals with evidence of a spiral growth mechanism. (B) At higher temperatures the smaller features of the sample disappear as premelting occurs preferentially at high energy edges and corners. In addition a phase separation occurs between different solid phases that are thought to be present at these temperatures. The lateral size of both images in the x and y directions is 11.4 μm .

high temperature that are virtually identical. Successful imaging requires the adjustment of the drive frequency at high temperatures to account for the resonance shift. In addition, though the free space amplitude of the tip may change with temperature, it is possible to correct for this by adjusting the drive voltage supplied to the cantilever. For example, by driving the cantilever shown in Fig. 5 at high drive voltages it is possible to increase the amplitude to the same level as at room temperature.

Once all of the instrumental changes in cantilever response are accounted for it is possible to use temperature control in TM-AFM to evaluate nanoscopic changes in soft materials. Figure 6 shows one example of many possible applications: the visualization of nanoscale changes in the melting of paraffin crystals. Figure 6(A) shows the room temperature image of $\text{C}_{33}\text{H}_{68}$ crystals grown on a flat silicon substrate. This material has a bulk melting point of $T_m = 72$ °C. The shape and form of the crystals are well known from electron microscopy experiments and represent the internal orthorhombic symmetry of the unit cell.^{23,28} At higher temperatures, Fig. 6(B), the crystals lose their high energy corners and the smaller plateaus disappear. In this particular case a phase separation is apparent in the image as the solid is near a solid–solid phase transition point. This example shows only one of the many applications of temperature con-

trol to TM-AFM used for topographic imaging. Temperature control would also be powerful when combined with numerous other TM-AFM imaging methods such as phase imaging and electric and magnetic force microscopy. While the heater presented here is technically suitable for these applications, the changes in microscope operation at high temperatures make interpretation and comparison of high and low temperature data more complex. This is the subject of ongoing work.

V. FINAL DISCUSSION

A simple hot stage can be built for a TM-AFM using a resistive heater and a commercially available temperature controller. This device reaches sample surface temperatures of 100 °C with no degradation in TM-AFM images or operation. A crucial issue in this heater design is the thermal insulation of the sample surface from the sample scanning stage. Without adequate insulation of the hot stage, images are distorted laterally. Insulation of the probe tip itself is not possible as it must contact the sample surface repeatedly. This changes the microscope operating conditions at high temperatures in predictable ways. To account for these changes and retain optimal imaging conditions the TM-AFM must be frequently retuned at high temperatures.

ACKNOWLEDGMENTS

We would like to acknowledge Deron Walters and Jason Cleveland for many helpful discussions, and Bruce Brinson for technical assistance. This work was supported by NSF-Chemistry (CHE-9702520) and the Welch Foundation (C-1342).

¹(a) M. Radmacher, R. W. Tillmann, M. Fritz, and H. E. Gaub, *Science* **257**, 1900 (1992); (b) G. Binnig, C. F. Quate, and C. Gerber, *Phys. Rev. Lett.* **56**, 930 (1986).

- ²L. A. Bottomley, J. E. Coury, and P. N. First, *Anal. Chem.* **68**, 185 (1996).
³(a) J. A. Zasadzinski, *Curr. Opin. Colloid Interface Sci.* **1**, 264 (1996); (b) Q. Zhong, D. Inniss, and V. B. Elings, *Surf. Sci.* **290** L688 (1993); (c) M. Radmacher, J. P. Cleveland, and P. K. Hansma, *Scanning* **17**, 117 (1995).
⁴D. Sarid, T. G. Ruskell, R. K. Workman, and D. Chen, *J. Vac. Sci. Technol. B* **14**, 864 (1996).
⁵B. Anczykowski, D. Kruger, K. L. Babcock, and H. Fuchs, *Ultramicroscopy* **66**, 251 (1996).
⁶N. A. Burnham *et al.*, *Nanotechnology* **8**, 67 (1997).
⁷J. P. Spatz, S. Sheiko, M. Moller, R. G. Winkler, P. Reinker, and O. Marti, *Nanotechnology* **8**, 40 (1995).
⁸T. Kajiyama, K. Tanaka, S. R. Ge, and A. Takahara, *Prog. Surf. Sci.* **52**, 1 (1996).
⁹S. Magonov and D. Reneker, *Annu. Rev. Mater. Sci.* **27**, 175 (1997).
¹⁰Z. Shao, J. Mou, D. M. Czajkowsky, J. Yang, and J.-Y. Yuan, *Adv. Phys.* **45**, 1 (1996).
¹¹Z. Shao and Y. Zhang, *Ultramicroscopy* **66**, 141 (1996).
¹²R. Euler, U. Memmert, and U. Hartmann, *Rev. Sci. Instrum.* **68**, 1776 (1997).
¹³H. Bluhm, S. H. Pan, L. Xu, T. Inoue, D. F. Ogletree, and M. Salmeron, *Rev. Sci. Instrum.* **69**, 1781 (1998).
¹⁴W. Allers, A. Schwarz, U. D. Schwarz, and R. Wiesendanger, *Rev. Sci. Instrum.* **69**, 221 (1998).
¹⁵S. Magonov, V. Elings, and V. Papkov, *Polymer* **38**, 297 (1997).
¹⁶I. Musevic, G. Slak, and R. Blinc, *Rev. Sci. Instrum.* **67**, 2554 (1996).
¹⁷T. R. Baekmark, T. Bjornholm, and O. G. Mouritsen, *Rev. Sci. Instrum.* **68**, 140 (1997).
¹⁸H. D. Sikes and D. K. Schwartz, *Science* **278**, 1604 (1997).
¹⁹C. T. Lynch, Ed. *Practical Handbook of Material Science* (CRC, New York, 1981), p. 108.
²⁰A. C. Company (personal communication).
²¹J. R. Shealy and G. W. Wicks, *Appl. Phys. Lett.* **50**, 1173 (1987).
²²N. A. Marigheto, E. K. Kemsley, J. Potter, P. S. Belton, and R. H. Wilson, *Spectrochim. Acta A* **52**, 1571 (1996).
²³I. M. Dawson and V. Vand, *Proc. R. Soc. London, Ser. A* **206**, 555 (1951).
²⁴G. Bar, Y. Thomann, R. Brandsch, H. J. Cantow, and M. H. Whangbo, *Langmuir* **13**, 3807 (1997).
²⁵S. N. Magonov, V. Elings, and M.-H. Whangbo, *Surf. Sci. Lett.* **375**, L385 (1997).
²⁶D. Kruger, B. Anczykowski, and H. Fuchs, *Ann. Phys. (Leipzig)* **6**, 341 (1997).
²⁷R. Brandtsch, G. Bar, and M.-H. Wangbo, *Langmuir* **13**, 6349 (1997).
²⁸E. B. Sirota, D. M. Singer, and H. H. Shao, *J. Chem. Phys.* **98**, 5809 (1993).